Supporting Information

Sikka et al. 10.1073/pnas.1420258111

SI Methods

The Johns Hopkins University Animal Care and Use Committee approved all protocols.

Vasoreactivity. Photorelaxation of blood vessels was assessed via force-tension myography in organ chambers (DMT). Mouse aortas were isolated and cleaned in ice-cold Krebs-Ringer-bicarbonate solution containing the following (in mM): 118.3 NaCl, 4.7 KCl, 1.6 $CaCl_2$, 1.2 KH_2PO_4, 25 $NaHCO_3$, 1.2 $MgSO_4$, and 11.1 dextrose. Vascular tension changes were determined as previously described (1). Briefly, one end of the aortic rings was connected to a transducer and the other to a micromanipulator. The aorta was immersed in a bath filled with constantly oxygenated Krebs buffer at 37 °C. Equal size thoracic aortic rings (2 mm) were mounted using a microscope, ensuring no damage to the smooth muscle or endothelium. At this point all lights were switched off, and the rest of the experiment was carried out in darkness with minimal red light turned on only for vision when required or when targeted wavelength light of certain intensity was used as part of the experiment. The aortas were passively stretched to an optimal resting tension using the micromanipulator, after which 60 mM KCl was administered, and repeated after a wash with Krebs buffer. After these washes the vessels were allowed to equilibrate for 20–30 min. Phenylephrine (1 μM) was administered to induce vasoconstriction. After a stable baseline was achieved, depending on the response required, wavelength doses were delivered via cold light lamp (Opelco 20500/06 by Fostec Inc.) (40,000–190,000 lux), light diodes [red (620–750 nm), green (495–570 nm), or blue (380–495 nm)] or a monochromator with varying wavelengths. SNP- or ACh-dependent dose responses were carried out as positive controls for SMC and endothelium activity, respectively. Responses were performed in the presence of inhibitors as determined by the experimental protocol. In this case, vessels were preincubated with the inhibitors for 30 min. Relaxation responses were calculated as a percentage of tension after preconstriction.

Laser Doppler Flowmetry. Procedures on animals were approved by the institutional animal care and use committee. Anesthesia was induced in male $Opn4^{+/+}$ and $Opn4^{-/-}$ with 5% (vol/vol) isoflurane and then was maintained with 1.5% (vol/vol) isoflurane. The mice were secured in the supine position with tape on the limbs. The ventral tail was cleaned with 70% (vol/vol) alcohol. A laser Doppler flow probe was placed on the ventral surface of the proximal portion of the tail. The position of the fiber-optic probe was adjusted to obtain a stable flux measurement and was secured in place with glue. A baseline flux was attained in 20 min in dark condition, after which the tail was exposed to blue light (455 nm at 40 lux) for 10 min, followed by a dark period of 10 min. Relative changes in red blood cell flux were monitored with a Perimed PeriFlux System 5000 Laser-Doppler flowmeter. Data were recorded every 15 s and are presented as percentage change from baseline.

Real-Time Quantitative PCR. Total RNA was extracted from isolated mice aortas using TRIzol and RNeasy Mini Kit (Qiagen) as described previously (2). RNA was then reverse transcribed with oligo dT primers to obtain cDNA using a SuperScript First Strand kit (Invitrogen), and quantitative real-time PCR (Applied Biosystems) was performed using SYBR Green Supermix mix (Applied Biosystems) and the following primer sets.

PCR was performed using mRNA isolated from mouse aortas of $Opn4^{+/+}$ and $Opn4^{-/-}$ mice using two sets of primers (for each target mRNA), used to amplify different product size:

Opn4 Set1	Forward 5′ CCCTGCTCATCATCATCTTCTG 3′
	Reverse 5′ TGACAATCAGTGCGACCTTGGC 3′
Opn4 Set2	Forward 5′ AGACGTTCTGAGTGCCGTTC 3′
	Reverse 5′ TTGCGCTTCATTGGACATTA 3′
PDE5A	Forward 5′ AATACCACCCCTGCAGCACC 3′
	Reverse 5′ TTCAAGGGCTCGCCAAAAGC 3′
PDE6G	Forward 5′ GAGCCCTGGGGAAGAAAC 3′
	Reverse 5′ CGGATGGAGTAGCTTAGTCTC3′

Adenovirus Encoding shRNA. Ad-sh-Nontargeted and Ad-shGRK2 (mice) encoded viruses were generated using a pAdBLOCK-iT kit (Life Sciences). Briefly, oligonucleotides targeting three different regions of mice GRK2 and nontargeted sequence were designed with proprietary software from Life Sciences and cloned into pU6-ENTR. Sequences used were as follows:

GRK2sh#A:

Top, 5′CACCGCAACACAGGGTACTACTTGACGAATCA-AGTAGTACCCTGTGTTGC3′

Bottom, 5′AAAAGCAACACAGGGTACTACTTGATTCGT-CAAGTAGTACCCTGTGTTGC3′

GRK2sh#B:

Top, 5′CACCGCCTTGAACACATGCACAATCCG AAGA-TTGTGCATGTGTTCAAGGC3′

Bottom, 5′AAAAGCCTTGAACACATGCACAATCTTCGG-ATTGTGCATGTGTTCAAGGC3′

GRK2sh#C:

Top, 5′CACCGGAGATCCAGTCAGTGGAAGACGAAT-CTTCCACTG ACTGGATCTCC3′

Bottom, 5′AAAAGGAGATCCAGTCAGTGGAAGATTC-GTCTTCCACTGACTGGATCTCC3′

Nontargeted:

Top, 5′CACCGATGGATTGCACGCAGGTTCTCGAAAG-AACCTGCGTGCAATCCATC3′

Bottom, 5′AAAAGATGGATTGCACGCAGGTTCTTTCGA-GAACCTGCGTGCAATCCATC3′.

The resulting pU6-sh-Nontargeted and pU6-GRK2shRNA plasmids were tested for correct sequence/orientation via Sanger sequencing (Johns Hopkins Medical Institution core) using U6 primer, and effectiveness of shRNA was tested in transient transfection experiments with mice embryonic fibroblast. The constructs showing the greatest inhibition was LR recombined with pAD/BLOCK-iTDEST (Invitrogen) to generate pAd-shGRK2. Adenoviruses were amplified and purified/concentrated using a Millipore Kit.

Western Blot Analysis. The aorta lysates were resolved by 10% (vol/vol) SDS/PAGE buffer, transferred, analyzed with antibodies, and visualized with peroxidase and an enhanced chemiluminescence system (Pierce).

E_m Measurements. Intracellular E_m recordings were performed in endothelium-denuded segments of murine thoracic aorta pinned in place lumen side down in a recoding chamber. The adventitia was removed and the tissue continuously perfused with Hepes-buffered saline solution containing (in mM): 130 NaCl, 5 KCl, 10 mM Hepes, 5 mM $MgCl_2$, 1.5 mM $CaCl_2$, and 10 mM glucose, with pH adjusted to 7.4 with 5 M NaOH and heated to 37 °C via an in-line heater (Warner Instruments). VSMCs were impaled with borosilicate glass microelectrodes (tip resistance 40–110 MΩ) that were fabricated on a Brown-Flaming P-87 electrode puller (Sutter Instruments) from thick-walled capillary tubes, filled with 3 M KCl, and connected to a current and voltage clamp amplifier (Axoclamp 2A; Axon Instruments). Intracellular recordings were performed in current clamp (3.0–4.0 kHz sampling rate) mode and recorded on a chart recorder (TA240; Gould Instrument Systems). Cellular recordings were accepted if the following were observed: (*i*) an abrupt negative deflection of potential as the microelectrode was advanced into a cell; (*ii*) stable membrane potential for at least 1 min; (*iii*) depolarization upon challenge with either KCl (60 mM) or PE (10μM); and (*iv*) an abrupt change in potential to ~0 mV after the electrode was retracted from the cell. During recording the entire experimental setup, including the tissue chamber and perfusate, was kept dark. Light challenge was achieved by exposure to the light emitted from a blue diode (380–495 nm) held directly above the recording chamber.

1. Mustafa AK, et al. (2011) Hydrogen sulfide as endothelium-derived hyperpolarizing factor sulfhydrates potassium channels. *Circ Res* 109(11):1259–1268.

2. Pandey D, et al. (2012) Expression and functional significance of NADPH oxidase 5 (Nox5) and its splice variants in human blood vessels. *Am J Physiol Heart Circ Physiol* 302(10):H1919–H1928.

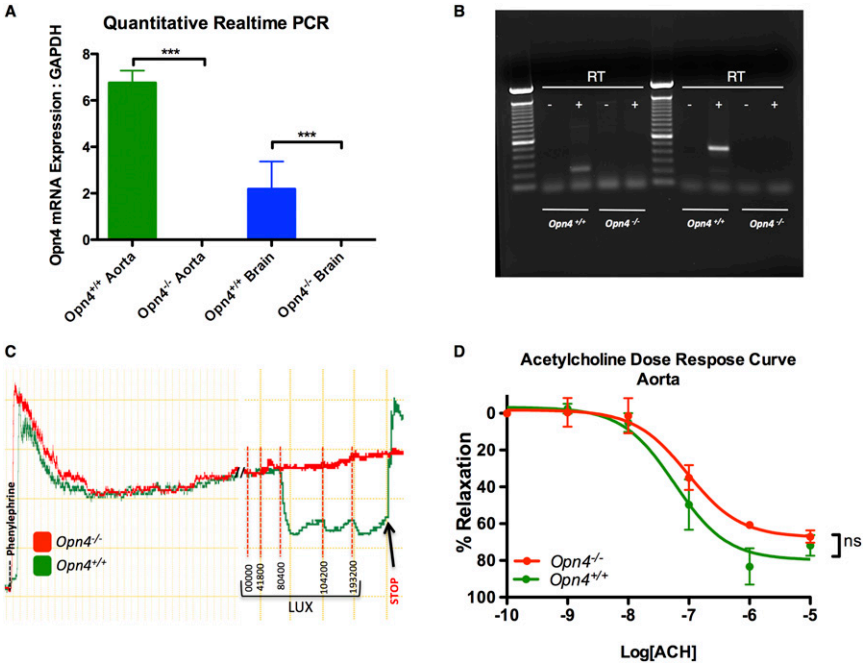

Fig. S1. (*A*) Quantitative real-time PCR analysis demonstrating abundance of Opn4 mRNA (Opn4 mRNA to GAPDH ratio) in aorta and brain of *Opn4*$^{+/+}$ mice compared with *Opn4*$^{-/-}$ negative controls. (*B*) RT-PCR analysis of mouse aorta using two separate primers sets demonstrates Opn4 mRNA expression in *Opn4*$^{+/+}$ mice but not *Opn4*$^{-/-}$ mice. $n = 6$. (*C*) Representative trace: vasoreactivity to cold white light demonstrates significant attenuation of photorelaxation in aortas from *Opn4*$^{-/-}$ mice compared with that of *Opn4*$^{+/+}$ mice. (*D*) Vasoreactivity: Cholinergic/acetylcholine dose–response curve demonstrating no difference in endothelial function in aortas isolated from *Opn4*$^{-/-}$ and *Opn4*$^{+/+}$ mice. $n = 4$.

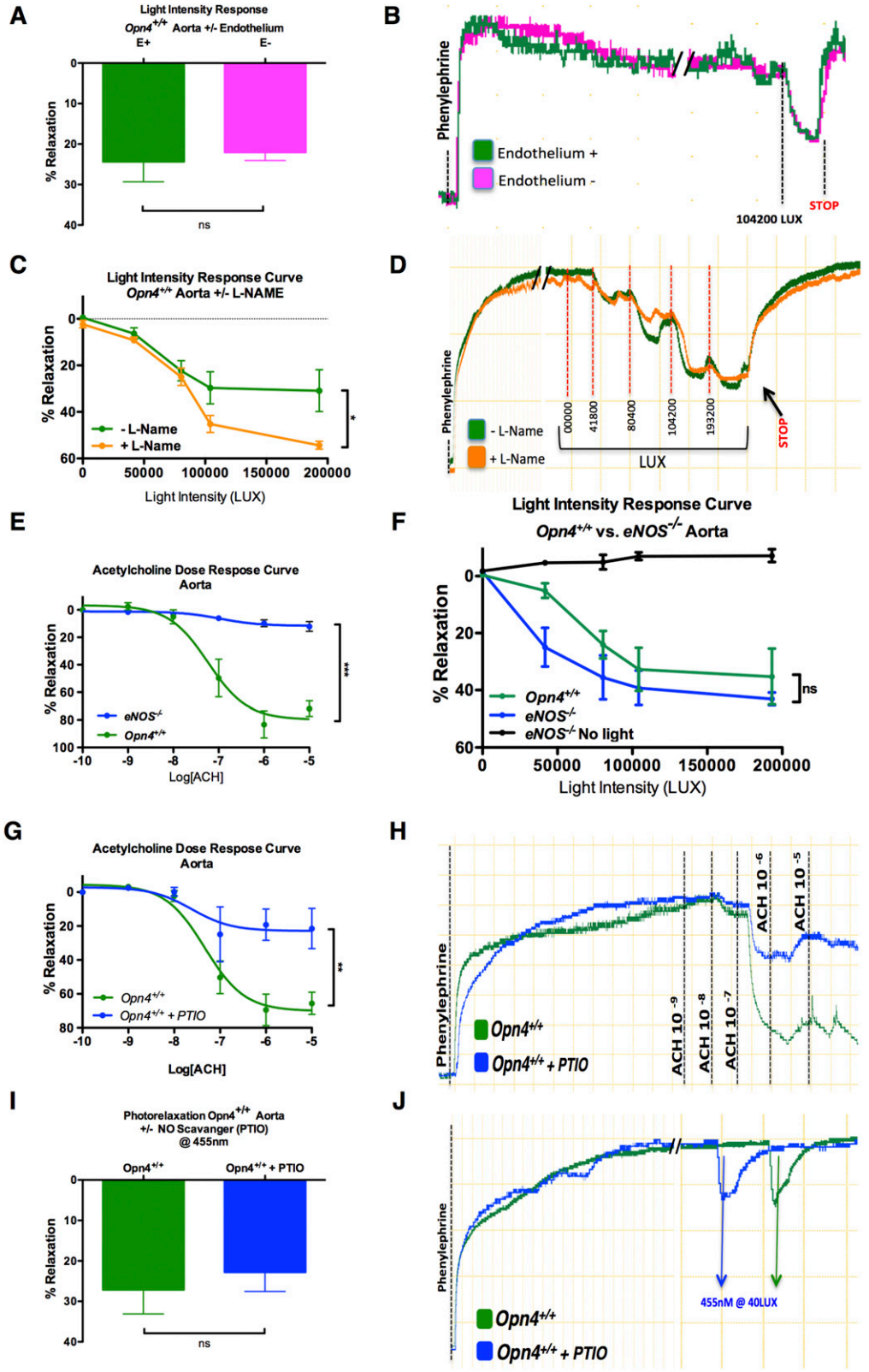

Fig. S2. (*A*) Vasoreactivity: cold white light repeat response demonstrates no difference in photorelaxation in endothelium-intact and endothelium-denuded *Opn4*$^{+/+}$ aorta ($n = 6$); and (*B*) associated representative trace. (*C*) Vasoreactivity: cold white light intensity response curve demonstrates a significant increase in photorelaxation in *Opn4*$^{+/+}$ aortas preincubated with the NOS inhibitor L-NAME (~54%) compared with untreated controls (~31%); and (*D*) associated representative trace. Error bars denote SEM, $n = 6$, $^{*}P < 0.05$. (*E*) Vasoreactivity: endothelial dependent/acetylcholine dose–response curves demonstrate a significant decrease in endothelial function (relaxation) in aortas isolated from *eNOS*$^{-/-}$ (12%) compared with ones isolated from *Opn4*$^{+/+}$ mice (72%). Error bars denote SEM, $n = 6$, $^{***}P < 0.001$. (*F*) Vasoreactivity: cold white light intensity response curve shows no difference in photorelaxation in aortas isolated from

Legend continued on following page

Opn4$^{+/+}$ and *eNOS*$^{-/-}$ mice. $n = 4$. (*G*) Vasoreactivity: endothelial dependent/acetylcholine dose–response curves demonstrate a significant decrease in endothelial function (relaxation) in *Opn4*$^{+/+}$ aortas preincubated with the NO scavenger CPTIO (~22%) compared with untreated controls (~66%); and (*H*) associated representative trace. Error bars denote SEM, $n = 6$, $^{**}P < 0.01$. (*I*) Vasoreactivity: light responses (455 nm at 40 lux) demonstrate no difference in photorelaxation in *Opn4*$^{+/+}$ aortas preincubated with the NO scavenger CPTIO compared with untreated controls ($n = 4$); and (*J*) associated representative trace.

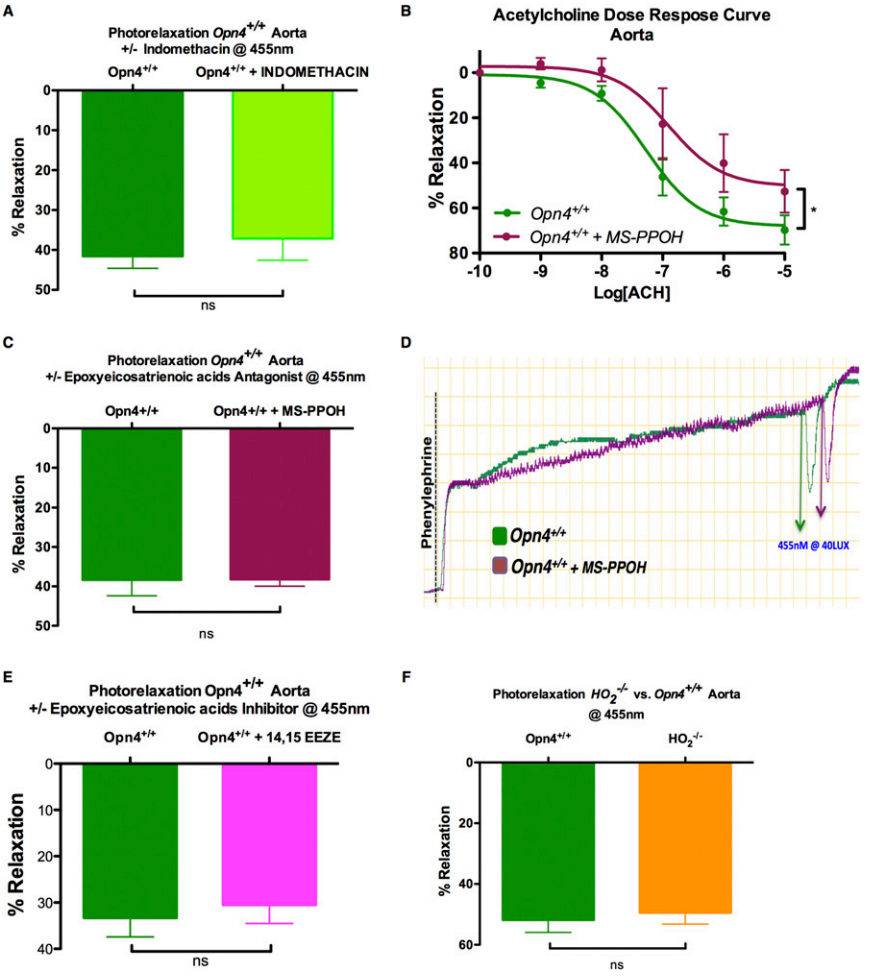

Fig. S3. (*A*) Vasoreactivity: light response (455 nm at 40 lux) demonstrates no difference in photorelaxation in *Opn4*$^{+/+}$ aortas preincubated with the cyclooxygenase inhibitor indomethacin compared with untreated controls. $n = 4$. (*B*) Vasoreactivity: endothelial dependent/acetylcholine dose–response curves demonstrates impaired endothelial function (relaxation) in *Opn4*$^{+/+}$ aortas preincubated with the EETs synthesis (cyp450 expoxygenase) inhibitor MS-PPOH and untreated controls. $n = 6$. (*C*) Vasoreactivity: light responses (455 nm at 40 lux) demonstrate no difference in photorelaxation in *Opn4*$^{+/+}$ aortas preincubated with MS-PPOH compared with untreated controls ($n = 6$); and (*D*) associated representative trace. (*E*) Vasoreactivity: light responses (455 nm at 40 lux) demonstrate no difference in photorelaxation in *Opn4*$^{+/+}$ aortas preincubated with EET synthesis inhibitor (14,15 EEZE) compared with untreated controls. $n = 11$. (*F*) Vasoreactivity: light responses (455 nm at 40 lux) show no difference in photorelaxation in aortas isolated from *Opn4*$^{+/+}$ compared with those isolated from *HO2*$^{-/-}$ mice. $n = 4$.

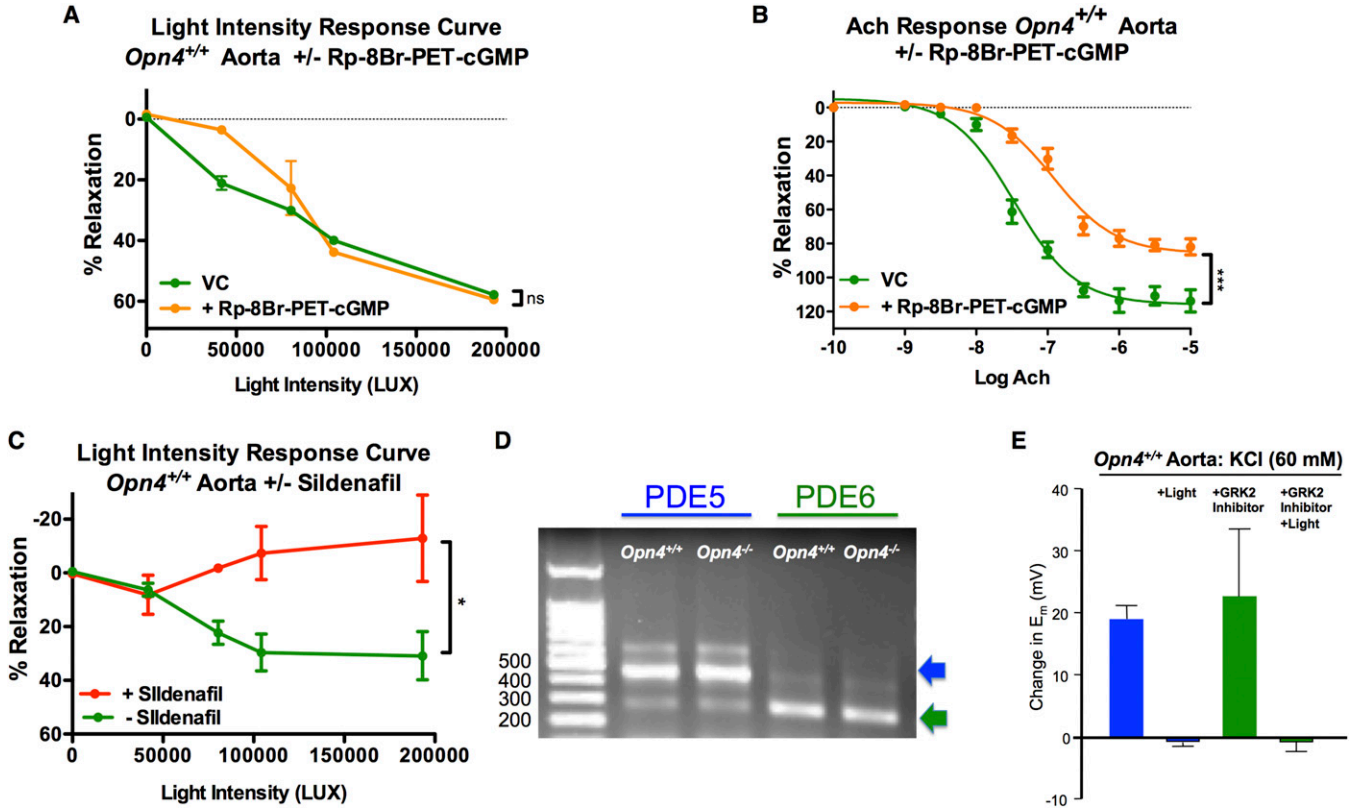

Fig. S4. (*A*) Vasoreactivity of *Opn4*$^{+/+}$ mouse aorta to cold white light demonstrates no significant difference in photorelaxation in vessels preincubated with the PKG inhibitor Rp-8Br-PET-cGMP compared with untreated vessels. $n = 3$. (*B*) Acetylcholine dose–responses in aortic rings preincubated with the PKG inhibitor Rp-8Br-PET-cGMP (10 μM), demonstrating impaired NO responses in Rp-8Br-PET-cGMP preincubated rings, but not VC. (All rings were incubated with indomethacin to inhibit cyclooxygenase-dependent non-NO hyperpolarizing factors). $n = 4$, $^{***}P < 0.001$. (*C*) Vasoreactivity: cold white light intensity response demonstrates a significant decrease in photorelaxation in *Opn4*$^{+/+}$ aortas preincubated with the PDE5 and PDE6 inhibitor sildenafil (~13%) compared with control aortic rings (~31%). Error bars denote SEM, $n = 3$ $^{*}P < 0.05$. (*D*) PCR analysis of mouse aortas demonstrates PDE5 and PDE6 mRNA expression in both *Opn4*$^{+/+}$ and *Opn4*$^{-/-}$ mice. $n = 6$. (*E*) Bar graph shows changes (mean ± SEM) in smooth muscle E_m in endothelium-denuded segments of mouse thoracic aorta under various conditions. E_m was measured in aortas from *Opn4*$^{+/+}$ mice perfused with KCl (60 mM) in the absence and presence of GRK2 inhibitor for 5 min in dark conditions before subjecting the tissue to light. $n = 5$–12.

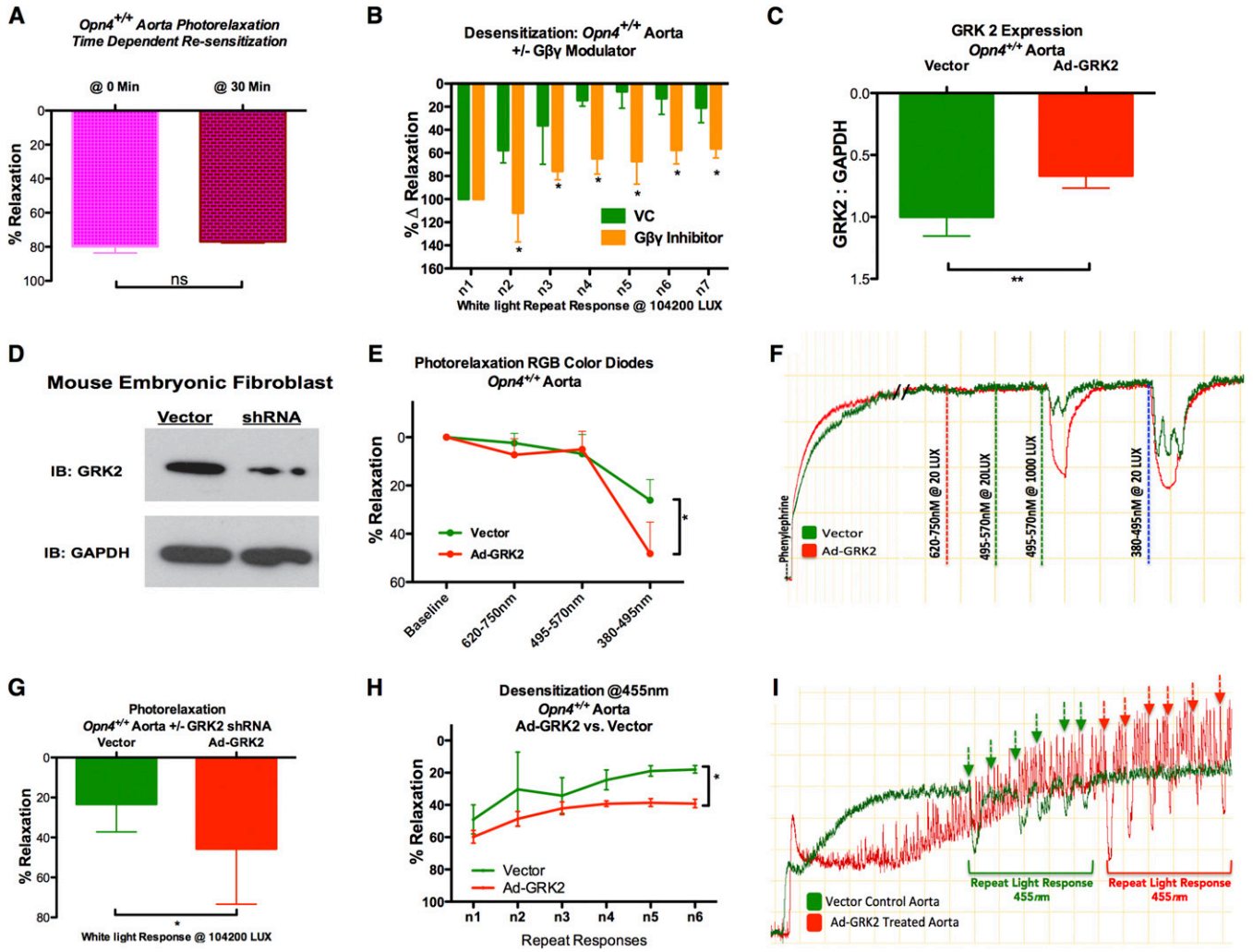

Fig. S5. (*A*) Vasoreactivity; *Opn4*$^{+/+}$ aortic ring data demonstrating time-dependent (~30 min) resensitization and resultant restoration of photorelaxation. $n = 2$. (*B*) Vasoreactivity: *Opn4*$^{+/+}$ aorta demonstrating desensitization/diminished vasodilatory responses to iso-intensity repeat light stimulation (cold white light at 104,200 lux) and attenuation of desensitization to same iso-intensity repeat light stimulation upon Gβγ inhibitor treatment. Error bars denote SEM, $n = 4$, $P < 0.01$. (*C*) Change in expression of GRK2 in *Opn4*$^{+/+}$ aortas treated with Ad-GRK2 adenovirus compared with vector control. $n = 6$. (*D*) GRK2 knockdown verification using mouse embryonic fibroblasts. (*E*) Vasoreactivity: *Opn4*$^{+/+}$ aortic rings, preincubated with the GRK2 shRNA adenovirus and vector adenovirus, demonstrate no relaxation to red (620–750 nm) and green (495–570 nm) wavelengths, whereas both groups demonstrate marked photorelaxation to blue (380–495 nm) light, which is significantly greater in the Ad-GRK2 group (~49%) compared with vector controls (~26%). Error bars denote SEM, $n = 3$, $^*P < 0.05$. (*F*) Representative trace, vasoreactivity of Ad-GRK2 vs. vector control *Opn4*$^{+/+}$ aorta to RGB wavelengths. (*G*) Vasoreactivity: cold white light response demonstrates increase in photorelaxation in the Ad-GRK2 group (~46%) compared with vector control (~23%) *Opn4*$^{+/+}$ aorta. Error bars denote SEM, $n = 3$, $^*P < 0.05$. (*H*) Vasoreactivity: *Opn4*$^{+/+}$ aorta demonstrating desensitization/diminished vasodilatory responses to iso-intensity repeat light stimulation (455 nm at 40 lux) and attenuation of desensitization/enhanced vasodilatory responses to the same iso-intensity repeat light stimulation upon GRK2 inhibition via Ad-GRK2 treatment. Error bars denote SEM, $n = 4$, $^*P < 0.05$. (*I*) Representative trace demonstrating desensitization resulting in loss of photorelaxation in vector-treated *Opn4*$^{+/+}$ aorta but lack of desensitization in AD-GRK2-treated *Opn4*$^{+/+}$ aortas, resulting in exaggerated vasodilatory responses with repeat blue light (455 nm at 40 lux) stimulations.